Applied Surface Science 406 (2017) 122–127

Contents lists available at ScienceDirect

Applied Surface Science

journal homepage: www.elsevier.com/locate/apsusc

Adsorbate-induced modification of electronic band structure of epitaxial Bi(111) films

A.V. Matetskiy[a,*], L.V. Bondarenko[a], A.Y. Tupchaya[a], D.V. Gruznev[a], S.V. Eremeev[b,c], A.V. Zotov[a,d,e], A.A. Saranin[a,d]

[a] Institute of Automation and Control Processes FEB RAS, 5 Radio Street, 690041 Vladivostok, Russia
[b] Institute of Strength Physics and Materials Science, 634021 Tomsk, Russia
[c] Tomsk State University, 634050 Tomsk, Russia
[d] School of Natural Sciences, Far Eastern Federal University, 690950 Vladivostok, Russia
[e] Department of Electronics, Vladivostok State University of Economics and Service, 690600 Vladivostok, Russia

ARTICLE INFO

Article history:
Received 4 November 2016
Received in revised form 16 January 2017
Accepted 6 February 2017
Available online 14 February 2017

Keywords:
Electron photoemission
Bismuth ultrathin films
Spin-splitting
Rashba effect

ABSTRACT

Changes of the electronic band structure of Bi(111) films on Si(111) induced by Cs and Sn adsorption have been studied using angle-resolved photoemission spectroscopy and density functional theory calculations. It has been found that small amounts of Cs when it presents at the surface in a form of the adatom gas leads to shifting of the surface and quantum well states to the higher binding energies due to the electron donation from adsorbate to the Bi film. In contrast, adsorbed Sn dissolves into the Bi film bulk upon heating and acts as an acceptor dopant, that results in shifting of the surface and quantum well states upward to the lower binding energies. These results pave the way to manipulate with the Bi thin film electron band structure allowing to achieve a certain type of conductivity (electron or hole) with a single spin channel at the Fermi level making the adsorbate-modified Bi a reliable base for prospective spintronics applications.

1. Introduction

Metal surfaces have been a prominent object for investigations of many basic condensed matter phenomena such as electron surface states, surface reconstructions, surface diffusion, etc. Nowadays metal surfaces still attract considerable attention. One such a topic deals with the spin-polarized surface states (SSs). The nature of spin–orbit splitting for these surface states is proved to be similar to the one of the Rashba–Bychkov effect in the semiconductor heterostructures and relies on the potential gradient originated from the asymmetry of the wave functions near the atom nuclei [1].

Among the metal surfaces, the Rashba effect was first observed at Au(111) [2]. Then it has consequently been found at the adsorbate-covered metallic surface [3–6], surface alloys [7], quantum well states (QWSs) in thin films [8,9] and metal-induced reconstructions on the semiconductor surfaces [10–13]. Together with the topological insulators [14], such materials are promising for use in spintronic devices. However, one needs techniques to control electronic properties of these novel materials, such as position of Fermi level, number and character of bands crossing it, magnitude of splitting, carrier density, etc.

It has been found that splitting values as well as Fermi level position can be varied through modifying the potential gradient by alkali metal and rare gas adsorption [15] or alloying [16,17]. But, it turns out that a result of such modifications is not universal and depends on the sign of the potential gradient of initial surfaces [18] being more pronounced for the surfaces of heavier elements [3].

Bismuth surface attracts intense attention due to its remarkable properties, including pronounced spin-splitting of the surface state bands [19–21] and clear manifestation of the quantum size effects [21]. Interplay between Rashba and quantum size effects, in turn, leads to the peculiar polarization dependence of surface states on the **k** vector [22] and on the thickness of the film [23]. Furthermore, depending on thickness Bi films undergo allotropic transformation [24] and semimetal-to-semiconductor transition [25,26].

In the present paper, we report on the modifications of the electronic structure of extrathin Bi films on Si(111) induced by cesium and tin adsorption. We have found that behavior of these adsorbates differs from the incorporation scenario observed for 3*d* transition metals [27]. Thus, Cs forms an adatom gas and alkali atoms donate electrons to the surface leading to shift of QWSs and SSs to the higher binding energies. Meanwhile, splitting of the sur-

* Corresponding author.
E-mail address: mateckij@iacp.dvo.ru (A.V. Matetskiy).

http://dx.doi.org/10.1016/j.apsusc.2017.02.023
0169-4332/

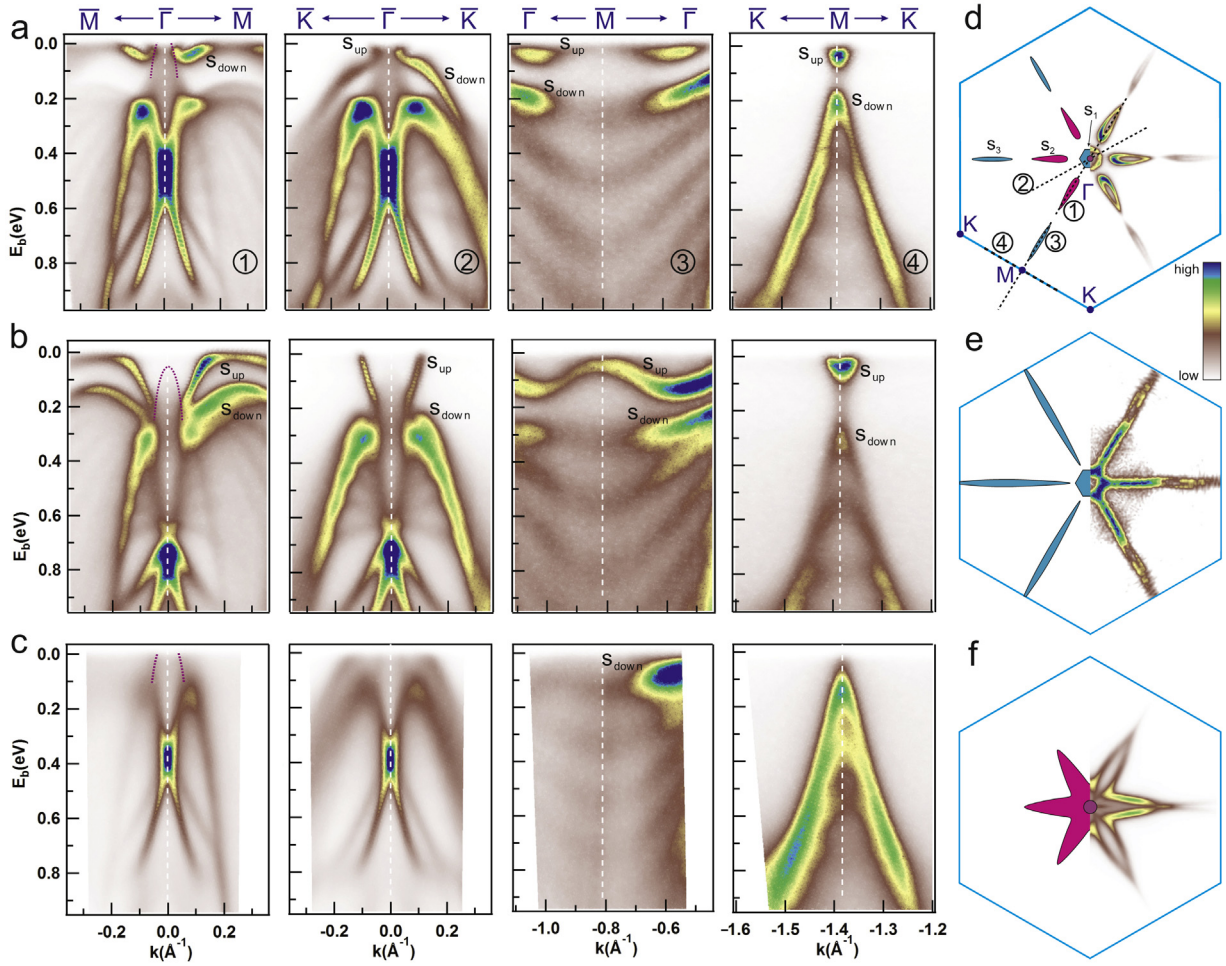

Fig. 1. ARPES spectra of (a) intact 14-BL-thick Bi film on Si(111), (b) the Bi film after RT deposition of ~0.1 mL of Cs and (c) after deposition of ~1.0 mL of Sn followed by annealing at 150 ° C. Position of the spectral cuts marked by numbers is indicated in the scheme of the Fermi surface of the intact Bi film in (d). Experimental Fermi surfaces (with their schematics given in the left half of SBZ) corresponding to the cases of (e) Cs and (f) Sn adsorption. Labels $\mathbf{s}_{up}$ and $\mathbf{s}_{down}$ mark upper and lower SS branches, respectively. The SS electron and hole pockets are colored in blue and pink, respectively and indicated by labels S_1, S_2 and S_3. Bulk hole pocket is colored in violet. Bulk band projection in $\bar{\Gamma}$ point in the (1) cut (left panels in (a), (b), and (c)) is outlined by the violet dotted line. (For interpretation of the references to color in this figure legend, the reader is referred to the web version of this article.)

face states increases. In contrast, tin atoms dissolve into the Bi film up to the limit of solubility and act as acceptor dopants.

2. Experimental and computational details

Experiments were conducted in the Omicron MULTIPROBE ARPES system operated in an ultrahigh vacuum ($\sim 2.5 \times 10^{-10}$ mbar). Scanning tunneling microscope (STM) images were obtained with Omicron variable temperature STM-XA using mechanically cut PtIr tips. Angle resolved photoemission spectroscopy (ARPES) measurements were performed using VG Scienta R3000 electron analyzer and high-flux He discharge lamp ($h\nu = 21.2$ eV) with toroidal-grating monochromator as a light source. For ARPES measurements samples were cryogenically cooled down to 78 K.

An atomically clean Si(111)7 × 7 surface was prepared *in situ* by flashing to 1280 °C after the sample was first outgassed at 600 °C for several hours. Bismuth was deposited from a Knudsen cell. Cesium was deposited from a well-outgassed commercial SAES chromate dispenser. Tin was deposited from the tantalum boat.

Electronic structure calculations were carried out within density functional theory (DFT) with using the Vienna Ab Initio Simulation Package (VASP) [28]. The interaction between the ion cores and valence electrons was described by the projector augmented-wave (PAW) method [29,30]. Relativistic effects, including spin–orbit interaction (SOI), were taken into account. For this calculations the PBE exchange-correlation functional [31] was used. The bulk Bi parameters were optimized and then they were used in slab calculations. In slab calculations on a slab of six bilayers with vacuum space of 15 Å was included to ensure negligible interaction between opposite surfaces. *k*-point meshes of 7 × 7 × 7 and 9 × 9 × 1 were used for the bulk and slab calculations, respectively. The total-energy convergence was better than 1×10^{-6} eV.

The bismuth film was prepared using the routine procedure which consists of the room temperature deposition of Bi onto Si(111)7 × 7 surface and subsequent annealing of the obtained film at 150 °C [32]. For the films thicker then ~6 bi-layers (1 BL = 1.14×10^{15} cm^{-2}), when phase transformation from black phosphorus phase to hexagonal phase takes place [24], such a procedure leads to the formation of a flat single-crystalline hexagonal Bi(111) film.

3. Results and discussion

The ARPES data on the band dispersion and Fermi map for the 14-BL thick Bi(111) film are shown in Fig. 1a and d, respectively. The spectral cuts in Fig. 1a correspond to the red dotted lines in the Fermi surface scheme in Fig. 1d. In agreement with previously

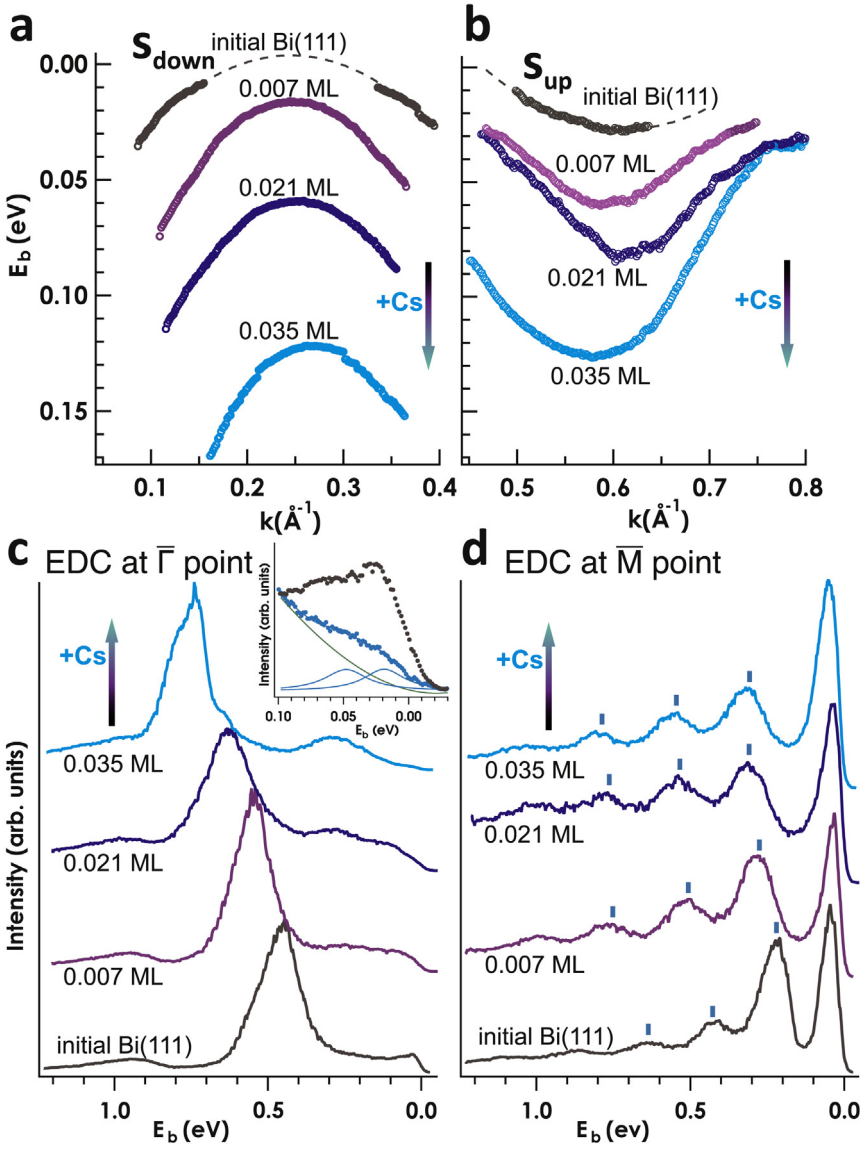

Fig. 2. Dispersion of the (a) $\mathbf{s}_{down}$ band and (b) $\mathbf{s}_{up}$ band in the $\bar{\Gamma}$–$\bar{M}$ direction (cut 1 and cut 3 in Fig. 1, respectively) for different Cs coverage. Energy distribution curves (EDC) (c) at the $\bar{\Gamma}$ and (d) $\bar{M}$ points for different Cs coverages. The trend of increasing Cs coverage is indicated by the arrow and corresponding color of the curves. The inset in (c) shows close look of the EDC near the Fermi level together with fitting results for spectrum profile of Cs modified film (blue lines). Green line marks the background. (For interpretation of the references to color in this figure legend, the reader is referred to the web version of this article.)

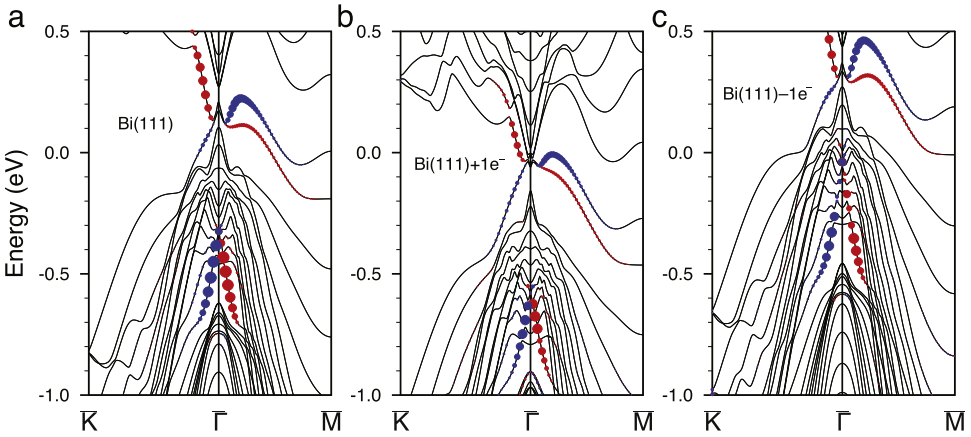

Fig. 3. Calculated electron band structure along the $\bar{K}$–$\bar{\Gamma}$–$\bar{M}$ direction for (a) relaxed Bi(111) slab and Bi(111) slabs with (b) additional and (c) missing electron. Surface states with opposite spin directions are marked by red and blue circles. (For interpretation of the references to color in this figure legend, the reader is referred to the web version of this article.)

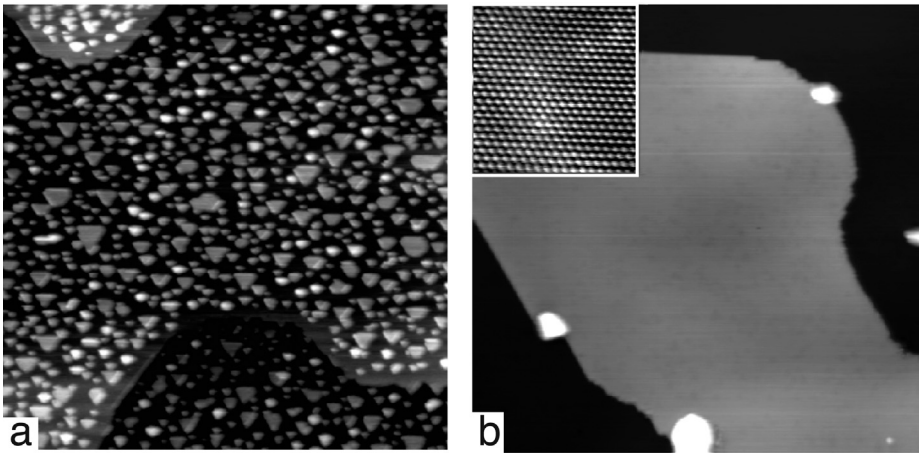

Fig. 4. 100 nm × 100 nm STM images of (a) ~1.0 mL of Sn deposited at room temperature and (b) annealed at 150 °C. Inset in (b) shows the surface structure with a greater magnification.

reported data, the surface states are presented by two branches marked as $\mathbf{s}_{up}$ and $\mathbf{s}_{down}$. The upper branch $\mathbf{s}_{up}$ forms sixfold electron pocket S_3 close to the $\bar{M}$ point and electron pocket S_1 at $\bar{\Gamma}$ point, when the lower branch $\mathbf{s}_{down}$ forms sixfold hole pocket S_2 in between $\bar{\Gamma}$ and $\bar{M}$. The results of the first-principles band calculations [19,20], as well as sp^3 tight-binding calculations [33] showed that these are the two branches of the spin-split band. It was found [22,34] that splitting is mostly of the Rashba-type, albeit out-of-plane component of spin approaches 25% of in-plane one, that is a result of the "intrinsic Bi crystal structure" [33]. In turn, the bulk band projection also crosses Fermi level in $\bar{\Gamma}$ point, where it forms tiny hole pocket [35]. Finally, as a result of quantum confinement in the film the QWSs appear. It was found that the hybridization among the surface and quantum well states forces the former one to lose their spin-split character near the $\bar{M}$ point (S_3 pocket) [20].

Room-temperature adsorption of Cs onto the Bi(111) films has been found to affect greatly the Bi electron band structure. Corresponding ARPES data for the highest Cs dose of ~0.1 mL are shown in Fig. 1b and e. Evolution of the different states with Cs dose is illustrated in Fig. 2. The general trend is that following Cs deposition SSs as well as bulk bands gradually shift to the higher binding energy (Fig. 2a). As a result $\mathbf{S}_{down}$ branch becomes fully located beneath the Fermi level and corresponding S_2 hole pocket disappears. At the same time, filling of the electron pockets S_1 and S_3 of the $\mathbf{s}_{up}$ branch increases (Fig. 1e).

The amount of energy shift, however, is not uniform and depends on band and $\mathbf{k}$ vector, that leads to the violation of shape of the SS branches. Thus, the extrema of $\mathbf{s}_{down}$ branch near the $\bar{\Gamma}$ point and $\mathbf{s}_{up}$ branch near the $\bar{M}$ point shift for up to 130 meV and 100 meV towards higher binding energy, respectively, as well as for up to 0.03 $Å^{-1}$ towards each other (Fig. 2a and b). Plausible the same effect takes place for the deep in-gap states at the center of Brillouin zone, which according to [21] also have a strong spin polarization (Fig. 2c). The crossing point in this case shift for almost 300 meV towards higher binding energies. The separation of the extrema of spin-split bands in $\mathbf{k}$ space could be attributed to the splitting parameter and hence the doping-induced modification of the spectrum is not confined to the rigid shift.

According to the very recent study of Ito et al. [37] the $\mathbf{s}_{up}$ branch is bounded to the conduction band minimum (CBM) at $\bar{M}$ point while $\mathbf{s}_{down}$ branch is bounded to the valence band, reflecting the non-trivial topology of Bi. Then, even though the bulk band is not clearly seen at the current photon energy we still can make a decision about CBM energy shift. According to the same study of Ito et al. [37] the CBM of 14-BL-thick locates almost exactly at the Fermi level. After Cs deposition $\mathbf{s}_{up}$ branch maximum at $\bar{M}$ point locates at 30 meV beneath the Fermi level. So, the energy shift of CBM should be closed to that value.

Similar estimation of bulk bands shift could be obtained from the energy distribution curve (EDC) at $\bar{\Gamma}$ point (Fig. 2c). One can notice disappearance of the characteristic Fermi-step feature in the profiles with Cs deposition. Data in the inset in Fig. 2c shows up a position of valence band maximum (VBM) at about 20 meV beneath Fermi level for Cs modified film. Taking into account it initial position [26], the energy shift of VBM should be of about 30–40 meV.

Finally, quantum-well states which is hybridized with SSs at $\bar{M}$ point [21] have similar to them shift towards the higher binding energies for ~100 to 150 meV, the effect being greater for the deeper states (Fig. 2d).

It has been found that the dose of 0.1 mL of Cs produces the greatest effect on the spectral features mentioned above and the effect vanishes at higher Cs coverages. However, STM observations at 0.1 mL of Cs have not revealed any specific features on the Bi(111) surface that could be associated with the presence of Cs adsorbate. They appear only at doses much higher than 0.1 mL of Cs as domains of the layer displaying $\sqrt{7} \times \sqrt{7}$ periodicity at the liquid nitrogen temperatures. As for 0.1 mL of Cs, the Cs adsorbate is plausibly present in the form of the 2D gas of mobile charged adatoms which could hardly be detected with STM due to tip effects. Charging of the Cs adatoms is believed to be a result of electronic charge transfer from the alkali-metal atom to the Bi film. Using DFT calculations, we have simulated semi-quantitatively this situation just by introducing one additional electron into the Bi slab. The results of simulations are shown in Fig. 3, where Fig. 3a shows the electron band structure of the intact Bi film and Fig. 3b that after adding an electron. One can see that the calculation results reproduce main trends observed in the ARPES experiments, namely an overall shift of the bands towards the higher binding energies as well as partial modification of the surface state dispersion owing to that the extra electron localized mainly at the surface layers.

Tin adsorption follows quite a different scenario both from the viewpoint of adsorbate interaction with a bismuth film and its effect on the electron band structure. Upon RT Sn adsorption, 2D islands of Bi-BL height are formed on the surface (Fig. 4a). However, annealing at 150 ° C restores a flat Bi(111) surface with a slightly modulated STM contrast (Fig. 4b). The other characteristic feature of such surface is a presence of seldom 3D islands. We speculate that Sn atoms dissolve into the Bi film bulk up to solubility limit (which is actually low [36]), while the excess Sn constitutes the

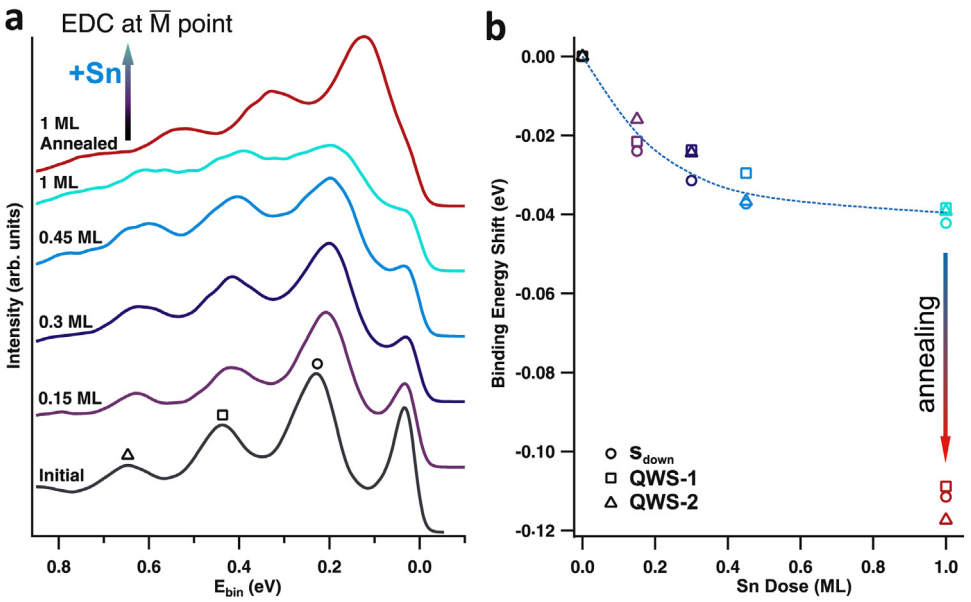

Fig. 5. (a) Evolution of the EDCs in the $\bar{M}$ point in the coarse of RT deposition of 0.15, 0.30, 0.45 and 1.0 mL of Sn and subsequent annealing at 150 °C. (b) Energy shifts of the EDC peaks, $\mathbf{s}_{down}$ bounded to valence band maximum (marked in (a) by circle) and two QWS peaks (marked in (a) by square and triangle) versus deposited Sn dose.

3D islands observed with STM. As for the change of the Bi electron band structure, Sn adsorption leads to decreasing electron band filling (Fig. 1c). The Fermi level gradually shifts downward with RT deposition in the range from 0.15 to 1.0 mL for ~40 meV as indicated by the rigid shift of all peaks in the energy distribution curves (Fig. 5b). Meanwhile, the spectra smear significantly (Fig. 5a). After annealing of the sample with 1.0 mL Sn at 150 °C, the Fermi level shifts further for additional ~70 meV, that seems to indicate a more complete electrical activation of Sn atoms dissolved in the Bi film bulk. The spectral features restore their sharpness due to improved crystal ordering of the film. Thus, Sn acts as an acceptor dopant, that it is quite natural bearing in mind that Sn and Bi are elements of Group IV and V, respectively. The S_2 hole pockets agglomerate into one star-like hole pocket, while the electron S_3 and S_1 pockets disappear (Fig. 1f). Bulk hole pocket at $\bar{\Gamma}$ point is expected to remain and enlarge in size, but it is difficult to find a clear confirmation for that in the ARPES spectra due to overlay and data smearing. The general changes in the Bi film spectrum after tin incorporation are well reproduced by the DFT calculations with missing electron (Fig. 3c), that simulates a hole doping.

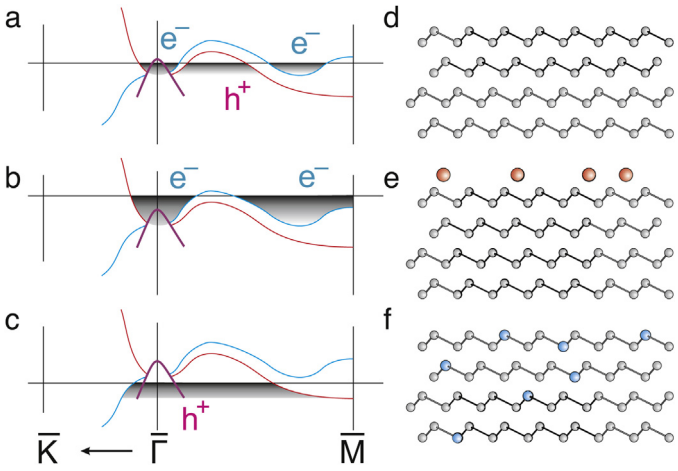

Fig. 6. Schematic view of surface state bands (shown by blue and red lines) and a bulk band (shown by violet line) along the $\bar{K}$–$\bar{\Gamma}$–$\bar{M}$ direction for (a) the intact Bi film and Bi films modified by (b) Cs and (c) Sn adsorption. Schematic structural models for (d) intact Bi film and Bi films modified by (e) Cs and (f) Sn adsorption. Bismuth, cesium, and tin atoms are shown by gray, red and blue circles, respectively. (For interpretation of the references to color in this figure legend, the reader is referred to the web version of this article.)

4. Conclusion

In conclusion, we present an efficient technique to modify the electron band structure of the epitaxial Bi(111) films in a desired manner using adsorption of appropriate species. Effects produced by adsorbates are illustrated in schematics shown in Fig. 6. In the band structure of the intact Bi film, both electron and hole pockets of the surface state bands are present (Fig. 6b and e). Upon RT adsorption of small amounts of Cs when it forms 2D adatom gas, the surface states shift to the higher binding energies by 100–300 meV due to electron charge transfer from Cs adsorbate to the Bi film. As a result, only the electron pockets are left at the Fermi surface (Fig. 6a and d). Bulk bands shift for ~30 meV. Upon RT adsorption of Sn followed by annealing at 150 °C, Sn atoms dissolve into the Bi film and act as acceptor dopant causing the shift of the Fermi level downward by ~100 meV. As a result, only the hole pockets are left at the Fermi surface (Fig. 6c and f). Since the surface state is spin split, the electron and hole doping as can be seen in Fig. 6 also leads to a switching off of one of the spin channels for surface conductivity that makes the doped Bi films potentially interesting for spintronics applications.

Acknowledgements

The present work was supported in part by the Grants NSh-6889.2016.2 and MK-5560.2016.2 of the President of the Russian Federation, Grants 15-02-02717 and 16-02-00505 of the Russian Foundation for Basic Research, and Grant 15-I-4-012 (0262-2015-0056) of the Russian Academy of Science Program "Far East".

References

[1] G. Bihlmayer, Y.M. Koroteev, P.M. Echenique, E.V. Chulkov, S. Blügel, The Rashba-effect at metallic surfaces, Surf. Sci. 600 (2006) 3888.

[2] S. LaShell, B. McDougall, E. Jensen, Spin splitting of an Au(111) surface state band observed with angle resolved photoelectron spectroscopy, Phys. Rev. Lett. 77 (1996) 3419.
[3] E. Rotenberg, J. Chung, S. Kevan, Spin–orbit coupling induced surface band splitting in Li/W(110) and Li/Mo(110), Phys. Rev. Lett. 82 (1999) 4066.
[4] M. Hochstrasser, J.G. Tobin, E. Rotenberg, S.D. Kevan, Spin-resolved photoemission of surface states of W(110)-(1 × 1)H, Phys. Rev. Lett. 89 (2002) 216802.
[5] M. Hoesch, M. Muntwiler, V.N. Petrov, M. Hengsberger, L. Patthey, M. Shi, M. Falub, T. Greber, J. Osterwalder, Spin structure of the Shockley surface state on Au(111), Phys. Rev. B 69 (2004) 1.
[6] A.M. Shikin, A.A. Rybkina, A.S. Korshunov, Y.B. Kudasov, N.V. Frolova, A.G. Rybkin, D. Marchenko, J. Sánchez-Barriga, A. Varykhalov, O. Rader, Induced Rashba splitting of electronic states in monolayers of Au, Cu on a W(110) substrate, New J. Phys. 15 (2013) 095005.
[7] C. Ast, J. Henk, A. Ernst, L. Moreschini, M. Falub, D. Pacilé, P. Bruno, K. Kern, M. Grioni, Giant spin splitting through surface alloying, Phys. Rev. Lett. 98 (2007) 186807.
[8] A. Varykhalov, J. Sánchez-Barriga, A.M. Shikin, W. Gudat, W. Eberhardt, O. Rader, Quantum cavity for spin due to spin–orbit interaction at a metal boundary, Phys. Rev. Lett. 101 (2008) 1.
[9] J.H. Dil, F. Meier, J. Lobo-Checa, L. Patthey, G. Bihlmayer, J. Osterwalder, Rashba-type spin-orbit splitting of quantum well states in ultrathin Pb films, Phys. Rev. Lett. 101 (2008) 1.
[10] K. Sakamoto, H. Kakuta, K. Sugawara, K. Miyamoto, A. Kimura, T. Kuzumaki, N. Ueno, E. Annese, J. Fujii, A. Kodama, T. Shishidou, H. Namatame, M. Taniguchi, T. Sato, T. Takahashi, T. Oguchi, Peculiar Rashba splitting originating from the two-dimensional symmetry of the surface, Phys. Rev. Lett. 103 (2009) 156801.
[11] I. Gierz, T. Suzuki, E. Frantzeskakis, S. Pons, S. Ostanin, A. Ernst, J. Henk, M. Grioni, K. Kern, C.R. Ast, Silicon surface with giant spin splitting, Phys. Rev. Lett. 103 (2009) 046803.
[12] K. Sakamoto, T. Oda, A. Kimura, K. Miyamoto, M. Tsujikawa, A. Imai, N. Ueno, H. Namatame, M. Taniguchi, P.E.J. Eriksson, R.I.G. Uhrberg, Abrupt rotation of the Rashba spin to the direction perpendicular to the surface, Phys. Rev. Lett. 102 (2009) 096805.
[13] K. Yaji, Y. Ohtsubo, S. Hatta, H. Okuyama, K. Miyamoto, T. Okuda, A. Kimura, H. Namatame, M. Taniguchi, T. Aruga, Large Rashba spin splitting of a metallic surface-state band on a semiconductor surface, Nat. Commun. 1 (2010) 17.
[14] M.Z. Hasan, C.L. Kane, Colloquium: topological insulators, Rev. Mod. Phys. 82 (2010) 3045.
[15] F. Forster, A. Bendounan, J. Ziroff, F. Reinert, Systematic studies on surface modifications by ARUPS on Shockley-type surface states, Surf. Sci. 600 (2006) 3870.
[16] C.R. Ast, D. Pacilé, L. Moreschini, M.C. Falub, M. Papagno, K. Kern, M. Grioni, J. Henk, A. Ernst, S. Ostanin, P. Bruno, Spin–orbit split two-dimensional electron gas with tunable Rashba and Fermi energy, Phys. Rev. B 77 (2008) 3.
[17] A. Crepaldi, G. Bihlmayer, K. Kern, M. Grioni, Combined large spin splitting and one-dimensional confinement in surface alloys, New J. Phys. 15 (2013) 105013.
[18] H. Bentmann, F. Reinert, Enhancing and reducing the Rashba-splitting at surfaces by adsorbates: Na and Xe on Bi/Cu(111), New J. Phys. 15 (2013) 115011.
[19] Y. Koroteev, G. Bihlmayer, J. Gayone, E. Chulkov, S. Blügel, P. Echenique, P. Hofmann, Strong spin–orbit splitting on Bi surfaces, Phys. Rev. Lett. 93 (2004) 046403.
[20] T. Hirahara, T. Nagao, I. Matsuda, G. Bihlmayer, E. Chulkov, Y. Koroteev, P. Echenique, M. Saito, S. Hasegawa, Role of spin-orbit coupling and hybridization effects in the electronic structure of ultrathin Bi films, Phys. Rev. Lett. 97 (2006) 146803.
[21] T. Hirahara, K. Miyamoto, I. Matsuda, T. Kadono, A. Kimura, T. Nagao, G. Bihlmayer, E. Chulkov, S. Qiao, K. Shimada, H. Namatame, M. Taniguchi, S. Hasegawa, Direct observation of spin splitting in bismuth surface states, Phys. Rev. B 76 (2007) 153305.
[22] T. Hirahara, K. Miyamoto, A. Kimura, Y. Niinuma, G. Bihlmayer, E.V. Chulkov, T. Nagao, I. Matsuda, S. Qiao, K. Shimada, H. Namatame, M. Taniguchi, S. Hasegawa, Origin of the surface-state band-splitting in ultrathin Bi films: from a Rashba effect to a parity effect, New J. Phys. 10 (2008) 083038.
[23] A. Takayama, T. Sato, S. Souma, T. Oguchi, T. Takahashi, Tunable spin polarization in bismuth ultrathin film on Si(111), Nano Lett. 12 (2012) 1776.
[24] T. Nagao, J. Sadowski, M. Saito, S. Yaginuma, Y. Fujikawa, T. Kogure, T. Ohno, Y. Hasegawa, S. Hasegawa, T. Sakurai, Nanofilm allotrope and phase transformation of ultrathin Bi film on Si(111)-7×7, Phys. Rev. Lett. 93 (2004) 105501.
[25] V.B. Sandomirskii, Quantum size effect in a semimetal film, Sov. Phys. JETP 25 (1967) 101.
[26] T. Hirahara, T. Shirai, T. Hajiri, M. Matsunami, K. Tanaka, S. Kimura, S. Hasegawa, K. Kobayashi, Role of quantum and surface-state effects in the bulk Fermi-level position of ultrathin Bi films, Phys. Rev. Lett. 115 (2015) 106803.
[27] C. Klein, N.J. Vollmers, U. Gerstmann, P. Zahl, D. Lükermann, G. Jnawali, H. Pfnür, C. Tegenkamp, P. Sutter, W.G. Schmidt, M. Horn-von Hoegen, Barrier-free subsurface incorporation of 3d metal atoms into Bi(111) films, Phys. Rev. B 91 (2015) 195441.
[28] G. Kresse, J. Hafner, *Ab initio* molecular dynamics for liquid metals, Phys. Rev. B 47 (1993) 558.
[29] P.E. Blöchl, Projector augmented-wave method, Phys. Rev. B 50 (1994) 17953.
[30] G. Kresse, D. Joubert, From ultrasoft pseudopotentials to the projector augmented-wave method, Phys. Rev. B 59 (1999) 1758.
[31] J.P. Perdew, K. Burke, M. Ernzerhof, Generalized gradient approximation made simple, Phys. Rev. Lett. 77 (1996) 3865.
[32] S. Yaginuma, T. Nagao, J.T. Sadowski, A. Pucci, Y. Fujikawa, T. Sakurai, Surface pre-melting and surface flattening of Bi nanofilms on Si(111)-7×7, Surf. Sci. 547 (2003) L877.
[33] K. Saito, H. Sawahata, T. Komine, T. Aono, Tight-binding theory of surface spin states on bismuth thin films, Phys. Rev. B 93 (2016) 041301.
[34] A. Kimura, E.E. Krasovskii, R. Nishimura, K. Miyamoto, T. Kadono, K. Kanomaru, E.V. Chulkov, G. Bihlmayer, K. Shimada, H. Namatame, M. Taniguchi, Strong Rashba-type spin polarization of the photocurrent from bulk continuum states: experiment and theory for Bi(111), Phys. Rev. Lett. 105 (2010) 13.
[35] Y. Liu, R.E. Allen, Electronic structure of the semimetals Bi and Sb, Phys. Rev. B 52 (1995) 1566.
[36] J. Vizdal, M.H. Braga, A. Kroupa, K.W. Richter, D. Soares, L.F. Malheiros, J. Ferreira, Thermodynamic assessment of the Bi–Sn–Zn system, Calphad 31 (2007) 438.
[37] S. Ito, B. Feng, M. Arita, A. Takayama, R.-Y. Liu, T. Someya, W.-C. Chen, T. Iimori, H. Namatame, M. Taniguchi, C.-M. Cheng, S.-J. Tang, F. Komori, K. Kobayashi, T.-C. Chiang, I. Matsuda, Proving nontrivial topology of pure bismuth by quantum confinement, Phys. Rev. Lett. 117 (2016) 236402.